Growth and characterisation of RbTiOPO$_4$:Nb crystals as a host for rare earth ions

J.J. Carvajal[a],*, R. Solé[a], Jna. Gavaldà[a], J. Massons[a], M. Rico[b], C. Zaldo[b], M. Aguiló[a], F. Díaz[a],*

[a]Laboratori de Física i Cristal·lografia de Materials, Universitat Rovira i Virgili, 43001 Tarragona, Spain
[b]Instituto de Ciencia de Materiales de Madrid, Consejo Superior de Investigaciones Científicas, Cantoblanco, 28049 Madrid, Spain

Abstract

The growth of RbTiOPO$_4$ crystals doped with Nb (RTP:Nb) by the Top Seeded Solution Growth (TSSG) technique is studied in order to obtain a suitable host for rare earths. Preliminary crystallographic and optical characterisations of these crystals show that the birefringence of the crystal increases with Nb incorporation, while the second harmonic generation capability is practically unmodified with respect to RTP. Moreover, a small but significant increase in the cut-off wavelength of the UV band edge with Nb incorporation is also found. Single crystals of RTP:Nb:Er and RTP:Nb:Yb by TSSG have been grown and no important changes with respect to the growth of RTP:Nb have been observed. The concentrations of rare earths achieved are $[Er^{3+}]=0.65\times10^{20}$ atoms·cm^{-3} and $[Yb^{3+}]=1.95\times10^{20}$ atoms·cm^{-3}. Polarised optical absorption spectra of Er^{3+} and Yb^{3+} in a RTP:Nb matrix are studied at 6 K and at room temperature. © 2001 Elsevier Science B.V. All rights reserved.

Keywords: Crystal growth; X-ray diffraction; Optical properties; Nonlinear optics

1. Introduction

Rubidium titanyl phosphate, RbTiOPO$_4$ (RTP), is an orthorhombic crystal, isostructural with the well known potassium titanyl phosphate, KTiOPO$_4$ (KTP), non-linear optical (NLO) crystal. Although less often used, RTP has NLO efficiency similar to that of KTP and it has also attracted a great attention as a NLO material [1,2]. Achieving self-induced effects by merging the laser properties of rare earth (RE) ions and the NLO properties of KTP has been hampered by the very low distribution coefficients of RE in KTP [3]. These distribution coefficients were slightly enhanced in RTP [4] but the RE concentration achieved was still far below that required for practical laser applications, namely about 10^{20} atoms·cm^{-3}.

In this work, we show that RE incorporation into RTP increases considerably when Nb is used as a co-doping element, giving spectroscopic evidence of Er^{3+} and Yb^{3+} incorporation. Moreover, we discuss the conditions suitable to the growth of RTP:Nb and RTP:Nb:Er or Yb crystals with optical quality by the Top Seeded Solution

Growth (TSSG) technique. Preliminary crystallographic and optical characterisations, like second harmonic generation (SHG) and refractive indices of the RTP:Nb host are also provided.

2. Crystal growth

Small single crystals of RTP:Nb and RTP:Nb:Er were obtained from solutions of the system Rb$_2$O–P$_2$O$_5$–TiO$_2$–Nb$_2$O$_5$–Er$_2$O$_3$. Basically, the solution composition was Rb$_2$O–P$_2$O$_5$–TiO$_2$=43.1–31.9–25 in mol%. For growing RTP:Nb crystals, part of the TiO$_2$ was substituted by Nb$_2$O$_5$, up to 3 mol% in the solution, and by Er$_2$O$_3$ or Yb$_2$O$_3$ when co-doping experiments were performed. Rb$_2$CO$_3$, NH$_4$H$_2$PO$_4$, TiO$_2$, Nb$_2$O$_5$, Er$_2$O$_3$ and Yb$_2$O$_3$ were used as starting materials. Solutions weighing about 15–25 g were prepared in conical, 25-cm^3 volume, platinum crucibles. Homogenisation was carried out while maintaining the temperature at about 50–100°C above the expected saturation temperature for 3–5 h. The axial temperature difference in the solution was about 8°C and the bottom of the solution was warmer than the surface. The temperature of the homogeneous solution was decreased at a rate of 10°C every 30 min until spontaneous crystallisation on a platinum wire immersed in the solution

---

*Corresponding author. Tel.: +34-977-55-9517; fax: +34-997-55-9563.

E-mail address: diaz@quimica.urv.es (F. Díaz).

was observed. To obtain transparent crystals of good enough quality for crystallographic and SHG studies, a 1.5 cm diameter Pt disc, rotating at 60 r.p.m., was immersed in the solution and the temperature was decreased by about 10°C at a rate of 0.5–1°C/h. After that, the crystals were removed slowly from the furnace to avoid cracks.

For spectroscopic studies and refractive indices measurements, high quality and larger single crystals of RTP:Nb and RTP:Nb:RE (RE=Er, Yb) were obtained by the TSSG technique. The solution composition for each growth experiment was basically the same as that used in the previous experiments, where part of the TiO_2 was substituted by Nb_2O_5, $Nb_2O_5+Er_2O_3$ or $Nb_2O_5+Yb_2O_3$, as shown in Table 1. Solutions with a weight of about 40 g were prepared in 25 cm^3 platinum crucibles. Crystal growth was carried out by decreasing the temperature by 15–30°C at a rate of 0.02–0.2°C/h from the temperature of saturation. Two RTP or RTP:Nb seeds displaced 4–5 mm from the rotation axis and rotating at about 65 r.p.m were used. The seeds were oriented with the *b* or *c* directions perpendicular to the surface of the solution and the *a* direction maintained in all cases in the radial position. In some of these experiments, an additional stir of the solution was used to propitiate the mass transport in the solution [5]. After the growth process, the crystals were slowly removed from the solution to minimise thermal stresses and the temperature of the furnace was decreased to room temperature at a rate of 15°C/h.

It is worth noting that the crystals obtained have a particular growth habit similar to that observed in KTP:Nb [6], i.e., their dimension in the *a* direction is significantly lower than that in *b* or *c* directions and the {1 0 0} face is more developed than the other crystal faces. On increasing the mass transport of the solution by stirring, the size difference between the *b* or *c* and *a* directions decreases.

Usually, when the concentration of Nb_2O_5 in the solution increases, some cracks beginning in the seed appear. To try to avoid these cracks, comparative growth attempts with RTP and RTP:Nb seeds were made. From these experiments, it was concluded that crystal cracks appear less often when RTP:Nb seeds are used, but at this stage, cracks could not be fully avoided. All these observations seem to indicate that the presence of Nb_2O_5 strongly influences the growth of RTP crystals. A more accurate

study of the positions of Nb^{5+} in the crystal is necessary in order to have a better understanding of the changes in the mechanism of growth.

3. Experimental characterisation

3.1. Dopant analysis

The dopant concentration in the crystals was analysed by Electron Probe Microanalyses (EPMA). A Cameca CAMEBAX SX-50 was used in wavelength dispersive mode operating at 25 kV accelerating voltage and 30 nA beam current for Nb, and 100 nA for Er and Yb. From these results and the solution composition used in every case, the distribution coefficients were calculated with the expression $K_x = ([X]/[Ti]+[Nb]+[RE])_{crystal}/([X]/[Ti]+[Nb]+[RE])_{solution}$ where X=Nb, Er or Yb and RE=Er or Yb. Table 1 summarises the results obtained. The RE concentrations achieved in the crystals are $[Yb^{3+}]=1.95 \times 10^{20}$ atoms·cm^{-3} for RTP:Nb:Yb and $[Er^{3+}]=0.65 \times 10^{20}$ atoms·cm^{-3} for RTP:Nb:Er. This Er concentration is one order of magnitude larger than that previously obtained in RTP grown without Nb_2O_5 [4]. The quality of the crystals is similar to that of RTP:Nb and these crystals show the same growth problems.

3.2. Crystallographic characterisation

The X-ray diffraction (XRD) data for the cell parameters refinement were collected using a Siemens D5000 powder diffractometer in a $\theta-\theta$ configuration using Bragg-Brentano geometry. The cell parameters were calculated from the diffraction data, obtained at $2\theta=10-70°$, step size (ss)=0.02°, step time (st)=16 s. The expansion coefficients were calculated from the patterns obtained at $2\theta=10-70°$, ss=0.03, st=5 s in the 25–425°C temperature range by collecting data every 100°C. In all cases, the FULLPROF program [7] and the Rietveld method [8] were used.

The evolution of the cell parameters and cell volume of RTP with Nb concentration was studied. While volume, and the *a* and *b* parameters decrease, *c* increases as the concentration of Nb increases. The evolution of these parameters with the temperature of a $RbTiOPO_4$ and a $RbTi_{0.94}Nb_{0.06}OPO_4$ was also analysed in the 25–425°C range. Similar behaviour is observed for this evolution in RTP and RTP:Nb, i.e. while the volume, and the *a* and *b* parameters increase with increasing temperature, *c* decreases. The results obtained for RTP agree well with the values in the literature [9].

The latter measurements allow the calculation of the thermal expansion coefficients given in Table 2. The RTP:Nb thermal expansion coefficients are slightly smaller than those observed for RTP (see Table 2), which implies a

Table 1
Distribution coefficients of Nb, Er^{3+} and Yb^{3+} in RTP grown using the TSSG method[a]

A	B	C	D	E
1	98–2–0–0	0.56		
2	94–6–0–0	0.49		
3	95–3–2–0	0.65	0.12	
4	94–3–0–3	0.60		0.37

[a] **A**: Experiment number. **B**: TiO_2–Nb_2O_5–Er_2O_3–Yb_2O_3 (mol%). **C**: Distribution coefficient of Nb. **D**: Distribution coefficient of Er. **E**: Distribution coefficient of Yb.

Table 2
Thermal-expansion coefficients (ppm/K)

	$RbTiOPO_4$	$RbTi_{0.945}Nb_{0.055}OPO_4$
α_{11}	12.7(2)	11.9(3)
α_{22}	17.7(5)	16.1(3)
α_{33}	−10.5(4)	−9.7(3)

lower thermal anisotropy. These results agree with the literature [9], taking into account that our results are averaged over a much smaller temperature range (25–425°C) than that used in the previous reference (20–700°C).

3.3. Optical characterisation of the host

Refractive index measurements of $RbTi_{0.94}Nb_{0.06}OPO_4$ were made by the minimum deviation angle using prisms [10]. To obtain the refraction indices along the three principal axes, two prisms with the mediatrix coincident with a principal plane (x–z for one prism and y–z for the other) were used, so the two refraction indices that we measure for each incidence beam corresponds to a principal axis value. The refraction indices were measured in the range 400–1500 nm using a narrow linewidth BMI VEGA Optical Parametric Oscillator pumped by a BMI SAGA seeded Nd:YAG laser.

Fig. 1 shows the dispersion chromatic curves of $RbTiOPO_4$ and $RbTi_{0.94}Nb_{0.06}OPO_4$ in the three principal directions. The results for RTP agree well with those found previously in the literature [11]. A significant increase in the three indices of RTP:Nb with respect to RTP can be observed as well as an enhancement of the birefringence. These results are similar to the birefringence changes of KTP:Nb crystals to respect KTP [12].

Dopants in KTP enhance the susceptibility to optical damage. This susceptibility to damage has been related to the growth of optical absorption bands close to the material's absorption edge in the ultraviolet region [13,14].
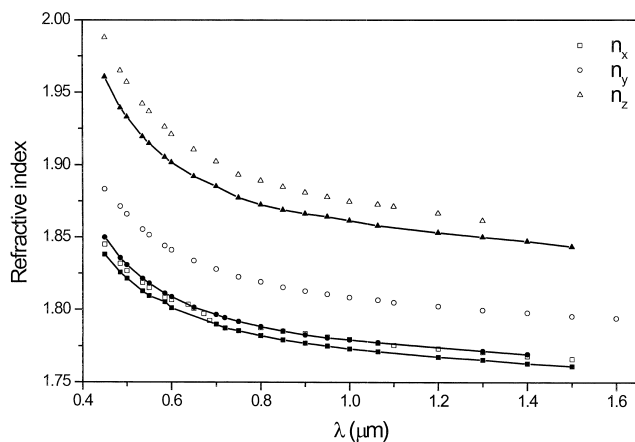
In order to observe this effect in our RTP:Nb samples, we have measured with a Varian Cary 500 Scan spectrophotometer the optical absorption of $RbTi_{1-x}Nb_xOPO_4$ ($x=0$ and 0.06) crystals. Spectra were collected at room temperature in the 350–500 nm range using non-polarised light propagating along the crystal a-axis. As grown, RTP:Nb crystals show broad bands in the visible region, similar to those observed in damaged or reduced KTP samples [15]. This broad absorption can be bleached by annealing at 500°C for 3 h. Fig. 2 shows the optical absorption after this annealing. The cut-off wavelength in the ultraviolet region of RTP:Nb is displaced to low energy with respect to RTP.

The SHG efficiency of RTP:Nb and RTP:Nb:Er were analysed using the Kurz powder technique [16] and were referred to KTP. For this purpose, crystalline samples were powdered, graded between 5 and 20 μm by standard sieves and loaded into a 2-mm-thick quartz cell. After that, they were illuminated with a Nd:YAG pulsed laser. The fundamental power at 1064 nm reflected and the back-scattered second harmonic power generated by the sample were collected and analysed using a digital oscilloscope. The ratio between the two signal intensities was used to describe the efficiency of the SHG process.

The RTP's SHG efficiency is practically unmodified with respect to KTP, as is expected from previous reports [17], and is maintained for RTP:Nb crystals. For the pumping and second harmonic wavelengths used, the possible losses due to Er^{3+} absorption were negligible.

3.4. Spectroscopy of RE dopants

The low temperature (6 K) optical absorption of Er^{3+} or Yb^{3+} in RTP:Nb crystals was determined with the spectrophotometer described previously and using a Leybold cryostat. The incident light beam was polarised parallel to the three crystallographic axes of the crystals.
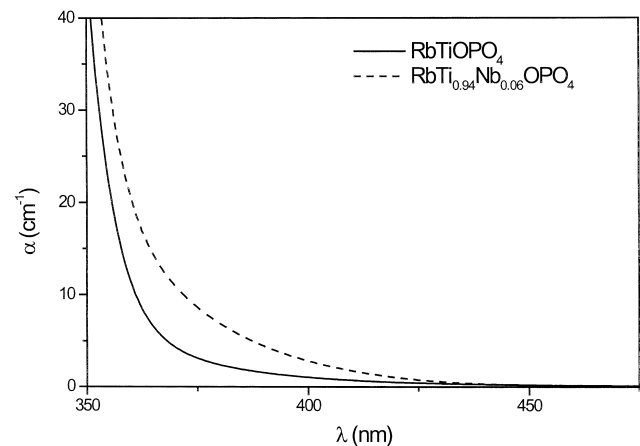
Fig. 3 shows polarised absorption spectra of Er^{3+} in a

Fig. 1. Dispersion and birefringence of $RbTi_{0.94}Nb_{0.06}OPO_4$. Solid lines are refractive indices of pure RTP.

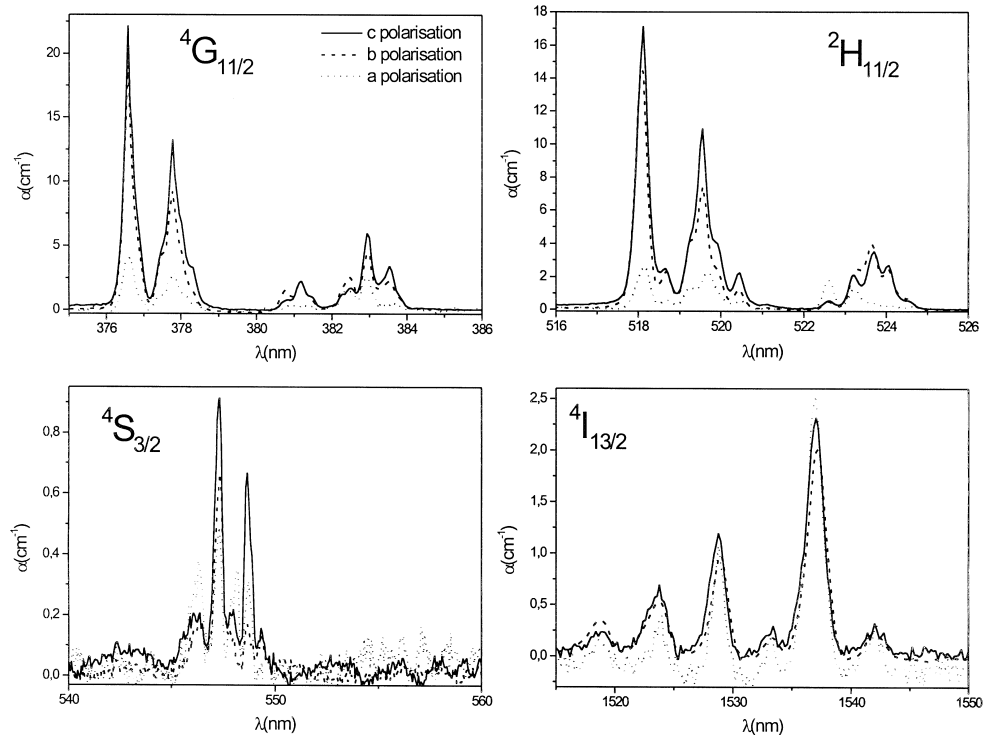Fig. 2. Evolution of the ultraviolet absorption edge of RTP with the concentration of Nb^{5+}.

Fig. 3. $^4G_{11/2}$, $^2H_{11/2}$, $^4S_{3/2}$ and $^4I_{13/2}$ multiplets of the polarised optical absorption spectrum of Er^{3+} in RTP:Nb obtained at 6 K.

$RbTi_{0.967}Nb_{0.026}Er_{0.007}OPO_4$ crystal that was previously annealed at 500°C for 3 h. The residual background absorption was analytically evaluated in the side regions of each multiplet and discounted from the spectra. Even though eleven $^{2S+1}L_J$ Er^{3+} multiplets, namely $^4G_{9/2}$, $^4G_{11/2}$, $^2H_{9/2}$, $^4F_{3/2}$, $^4F_{5/2}$, $^4F_{7/2}$, $^2H_{11/2}$, $^4S_{3/2}$, $^4F_{9/2}$, $^4I_{11/2}$ and $^4I_{13/2}$, can be clearly resolved, Fig. 3 shows only the most intense ones for the sake of brevity. Comparison of the present result on RTP:Nb:Er with those reported for RTP:Er [4] evidences the higher Er^{3+} concentration in the RTP:Nb:Er crystal. As can be seen in Fig. 3, this sample presents a strong dichroism. The spectra parallel to the c direction show a slightly higher intensity than the spectra collected parallel to the b direction; however, generally a strong reduction of the absorption coefficient is observed in the spectrum parallel to the a direction. It is suggested that Er^{3+} occupies the two non-equivalent Ti^{4+} positions of the structure differently. In RTP:Nb:Er, a displacement of the lines of each multiplet to higher wavelengths can be observed with respect to RTP:Er [4].

Fig. 4 shows the room temperature Yb^{3+} polarised absorption of $RbTi_{0.935}Nb_{0.043}Yb_{0.022}OPO_4$. The unique Yb^{3+} contribution in the 800–1100 nm range arises from the $^2F_{5/2}$ multiplet. Again, a strong dichroism was observed. Although the three peaks of this multiplet are observed in all spectra, strong differences between c and b polarisations exists: the intensity of the two side peaks of the multiplet are inverted. The a polarisation has a similar behaviour to b polarisation, but with a lower intensity. It must be finally mentioned that the intensity of the Yb^{3+}

absorption shown in Fig. 4 is about one order of magnitude larger than that achieved previously in $KTiOAsO_4$ crystals [18].

4. Conclusions

A preliminary characterisation of RTP:Nb shows that this matrix is a good host for rare earth ions. Single crystals of RTP:Nb:Er of optical quality were grown and the distribution coefficients of rare earths and Nb in the crystals were obtained. The crystals obtained have a particular growth habit similar to that observed in KTP:Nb.
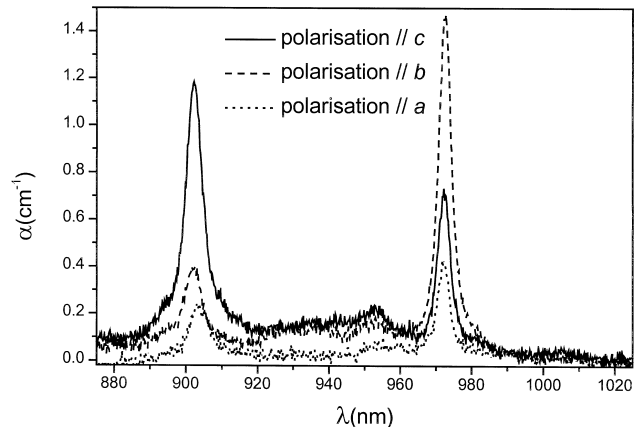

Fig. 4. Polarised optical absorption spectrum of Yb^{3+} in RTP:Nb at room temperature.

The use of Nb as co-doping produces an increase the distribution coefficient of RE, while maintaining the SHG properties, even when Er^{3+} is included in the matrix. The presence of Nb increases the birefringence of the crystal but slightly reduces the ultraviolet transparency of the host. Finally, the absorption bands of Er^{3+} and Yb^{3+} in this matrix were characterised using light polarised parallel to the *a*, *b* and *c* crystallographic axes, respectively. A strong dichroism was observed.

Acknowledgements

References

[1] J.Y. Wang, Y.G. Liu, J.Q. Wei, L.P. Shi, M. Wang, Zeitschrift für Kristallographie 191 (1990) 231.

[2] M.E. Hagerman, K.R. Poeppelmeir, Chem. Mater. 7 (1995) 602.

[3] R. Solé, V. Nikolov, I. Koseva, P. Peshev, X. Ruiz, C. Zaldo, M.J. Martín, M. Aguiló, F. Díaz, Chem. Mater. 9 (1997) 2745.

[4] M. Rico, C. Zaldo, J. Massons, F. Díaz, J. Phys. Condens. Matter. 10 (1998) 10101.

[5] J.J. Carvajal, V. Nikolov, R.J. Solé, Jna. Gavaldà, M. Massons, C. Rico, M. Zaldo, F. Aguiló, Díaz. Chem. Mater 12 (2000) 3171.

[6] J. Wang, Y. Liu, J. Wei, M. Jiang, Z. Shao, W. Liu, S. Jiang, Cryst. Res. Technol. 78 (1997) 319.

[7] J. Rodríguez-Carvajal, Short reference guide of the program FULLPROF, Laboratoire Leon Brillouin, 1998.

[8] R.A. Young, The Rietveld Method, Oxford Science Publication, International Union of Crystallography, 1995.

[9] P. Delarue, C. Lecomte, M. Jannin, G. Marnier, B. Menaert, Phys. Rev. B 58 (1998) 5287.

[10] T.Y. Fan, C.E. Huang, B.Q. Hu, R.C. Eckardt, Y.X. Fan, R.L. Byer, R.S. Feigelson, Appl. Optics 26 (1997) 2390.

[11] Y.S. Oseledchik, A.I. Pisarevsky, A.L. Prosvirnin, V.N. Lopatko, L.E. Kholodenkov, F.F. Titkov, A.A. Demidovich, A.P. Shkadarevich, in: Proc. of Lasers Optics Conf, Leningrad University Press, Leningrad, 1990.

[12] L.T. Cheng, L.K. Cheng, R.L. Harlow, J.D. Bierlein, Appl. Phys. Lett. 64 (1994) 155.

[13] M.J. Martín, C. Zaldo, F. Díaz, R. Solé, D. Bravo, F.J. López, Radiat. Eff. Defects Solids 136 (1995) 243.

[14] C. Zaldo, J. Carvajal, R. Solé, F. Díaz, D. Bravo, A. Kling, J. Appl. Phys. 88 (2000) 3242.

[15] M.J. Martín, D. Bravo, R. Solé, F. Díaz, F.J. López, C. Zaldo, J. Appl. Phys. 76 (1994) 7510.

[16] S.K. Kurz, T.T. Perry, J. Appl. Phys. 39 (1968) 3798.

[17] V.I. Voronkova, V.K. Yanovskii, Izvestiya Akademii Nauk SSSR Organicheskie Materialy 24 (1988) 273.

[18] A.P. Yelisseyev, L.I. Isaenko, A.I. Belov, A.A. Merkulov, J. Cryst. Growth 198/199 (1999) 555.